Biochimica et Biophysica Acta, 1106 (1992) 85–93

BBAMEM 75595

Glycosphingolipid phase behaviour in unsaturated phosphatidylcholine bilayers: a ^{2}H-NMR study

Michael R. Morrow [a], Dev Singh [b], Dalian Lu [a] and Chris W.M. Grant [b]

[a] *Department of Physics, Memorial University of Newfoundland, St. John's, Newfoundland (Canada)* and [b] *Department of Biochemistry, University of Western Ontario, London, Ontario (Canada)*

(Received 16 August 1991)
(Revised manuscript received 6 January 1992)

Key words: Glycolipid; Bilayer; Phase diagram; NMR, ^{2}H-

^{2}H-NMR was employed to consider the arrangement of a glycosphingolipid, *N*-(lignoceroyl-d_{47})galactosylceramide, in bilayers of the mono-unsaturated phospholipid, 1-stearoyl-2-oleoylphosphatidylcholine. The deuterated glycolipid prepared by partial synthesis was incorporated at concentrations ranging from 5 mol% to 53 mol% into unsonicated liposomes, and its spectra were recorded from +76°C to −3°C. First spectral moments were plotted as a function of temperature for each sample composition and, along with inspection of the spectra, were employed to infer a phase diagram describing glycolipid behaviour in the unsaturated phospholipid host matrix. It was possible to refine the result using ^{2}H-NMR difference spectroscopy. The phase diagram obtained was indicative of peritectic behaviour. At glycolipid concentrations exceeding about 20 mol% there was considerable tendency to glycolipid phase separation – as indicated by coexistence of fluid phospholipid-enriched and gel phase glycolipid-enriched domains over a wide range of temperatures, and by coexistence of distinct ordered phase domains at lower temperature. In contrast, at lower glycolipid concentrations reflective of many biological membranes, the lipid components were miscible in both the liquid crystal and gel phases, with only a narrow temperature range of fluid and ordered phase coexistence. For the fluid phase at low glycolipid concentrations, spectra of the deuterated glycolipid 24-carbon fatty acid suggest that orientational order is low for a number of methylene groups near the methyl end of the chain.

Introduction

Glycosphingolipids (GSLs) are the carbohydrate-bearing lipids of higher animal cells. They are known to be involved as recognition sites and structural elements of the plasma membrane. It has been observed that physical arrangement and motional characteristics of GSLs in membranes modulate their phenotypic expression as recognition sites, in addition to being determinants of their structural impact at the membrane surface [1–4]. Of particular value in understanding the forces that might underlie such phenomena have been experiments with pure GSLs, which lend themselves to detailed interpretation [1,5]. However scientists working with these systems have indicated that it is crucial to also investigate mixtures of glycolipids with other membrane components, in spite of the resultant much greater difficulties of interpretation. One instructive approach to dealing with this concern has been examination of the phase behaviour [6] of glycolipids in phospholipid membranes, since such experiments can be correlated with molecular arrangement and dynamics [1,3,4].

Amongst the earliest work on GSL phase behaviour in phospholipid host matrices was a DSC study by Bunow and Bunow of GM_1 and total brain gangliosides in mixtures with 1-stearoyl-2-oleoylphosphatidylcholine (SOPC) [7]. These complex, charged glycolipids having natural fatty acid composition appeared to be miscible with SOPC when they comprised less than 30 mol% of the lipid. Bach et al. recorded a calorimetric study of native GM_1 in egg phosphatidylcholine that demonstrated complete miscibility [8]. Maggio et al. systematically examined a series of neutral and charged GSLs, having natural fatty acid composition, in bilayers of dipalmitoylphosphatidylcholine (DPPC) [9]. They observed considerable dependence of their phase dia-

Abbreviations: GSL, glycosphingolipid; SOPC, 1-stearoyl-2-oleoylphosphatidylcholine; GalCer, Galβ1 → 1ceramide; DPPC, dipalmitoylphosphatidylcholine.

Correspondence: M.R. Morrow, Department of Physics, Memorial University of Newfoundland, St. John's, Newfoundland, Canada A1B 3X7 and C.W.M. Grant, Department of Biochemistry, University of Western Ontario, London, Ontario, Canada N6A 5C1.

grams on GSL characteristics such as charge and carbohydrate composition; but in general the regions of low glycolipid concentration showed horizontal solidus curves suggesting solid phase immiscibility. GSL fatty acid structure has been mentioned as a factor to consider in such studies [1,2]. It differs from that of phospholipids in that the common GSL fatty acids found within a given membrane are from 18 to 24 carbons, vs. 16 to 18 for phospholipids. Furthermore, the 'typical' cell membrane phospholipid has a *cis* mono-unsaturated fatty acid at the glycerol 2-position; with the result that the phase transition temperature of such a lipid is some 40°C lower than that of DPPC (41.5°C) (GSLs generally have very high phase transition temperatures, in the range 50–85°C [10].). Hence, it has been pointed out that one important extension of glycolipid studies is to GSL/phosphatidylcholine mixtures in which the glycolipid fatty acid is longer than that of the host matrix, and in which the host matrix lipids are not fully saturated [1,11].

DSC is sensitive to phase changes, which in turn are determined by the molecular properties of the sample as a whole. In the present study we have considered the utility of ^{2}H-NMR for following GSL phase behaviour in a host matrix by employing a spectroscopic probe which was part of the glycolipid structure. This approach offers certain potential advantages in that GSLs are often very minor membrane components: we were able to study in detail the biologically important low GSL concentration region of the phase diagram by monitoring spectral shape as a function of temperature. A technique of spectral subtraction was used which permitted additional refinement of phase boundaries [12–14]. We have focused on the glycolipid, *N*-(lignoceroyl)galactosylceramide (*N*-(lignoceroyl) GalCer), having homogeneous (24:0) fatty acid composition. As host matrix we selected SOPC, which has 18-carbon fatty acids. The main transition for SOPC occurs at 6°C [15]; it was chosen in preference to 1-palmitoyl-2-oleoylphosphatidylcholine (POPC) which undergoes a main transition at −3°C, since the latter is in the range over which water freezes in liposome suspensions – an event that may influence detection of simultaneous processes in suspended lipid.

GalCer is an important GSL which has been the subject of earlier investigations. In particular, properties of pure *N*-(lignoceroyl)GalCer in fully hydrated form are known from DSC and X-ray diffraction work [16]. It displays a fluid/gel main transition at 82°C, and exhibits metastable polymorphism at lower temperatures [16]. A phase diagram has been derived for *N*-(palmitoyl)GalCer/DPPC [17], which is characterised by solid phase immiscibility and a considerable temperature range of fluid/gel phase coexistence at GSL fractions greater than 0.2. The corresponding DSC-derived phase diagram for *N*-(lignoceroyl) GalCer/DPPC displayed solid phase immiscibility over the entire composition range [18]. Phase diagrams for GalCer with natural beef brain fatty acid composition have also been derived in DPPC [9] and in POPC [11] host matrices. In the former, the solidus was horizontal to a GSL mol fraction of 0.4 and the fluidus close to horizontal to 0.3. In the latter, the phase diagram showed solid phase immiscibility, and striking phase separation of coexisting fluid (phospholipid-enriched) and rigid (glycolipid-enriched) domains over a wide range of temperature and composition, extending to membranes with very low glycolipid content.

Materials and Methods

1-Stearoyl-2-oleoylphosphatidylcholine (SOPC) and galactosylceramide (GalCer, from beef brain) were obtained from Avanti Polar Lipids, Birmingham, AL; and were used without further purification. LysoGalCer (i.e. GalCer from which the fatty acid had been removed) was produced from the above material by hydrolysis in refluxing butanolic KOH as has been described previously [19,20]; and was purified before use on a column of silicic acid (Bio-Rad 200–400 mesh), eluting with a gradient of methanol in chloroform. Reactions were followed on Merck silica gel 60 thin-layer chromatography plates eluted with 65 : 15 $CHCl_3/CH_3OH$ and developed with sulfuric acid/ethanol spray. *N*-(Lignoceroyl-d_{47})GalCer was made by converting 31.0 mg (74.5 μmol) of perdeuterated lignoceric acid (Aldrich) to the acid chloride, and subsequently combining this with 32.0 mg (67.1 μmol) of lysoGalCer [21]. Purification was by silicic acid column chromatography eluting with a chloroform/methanol gradient, as for the lyso compound – yield 55% (31.8 mg (37.0 μmol)) of deuterated GSL. GalCer with 24-carbon fatty acid co-migrated with the faster-running spot of native beef brain GalCer.

Mixtures of *N*-(lignoceroyl-d_{47})GalCer in SOPC were prepared with glycolipid concentrations of 53 mol%, 35 mol%, 24 mol%, 10 mol% and 5 mol%. Because of the limited amount of deuterium-labelled GalCer available, it was necessary to reclaim each sample and use it in preparation of the next. The dry components were co-dissolved in ethanol which was then removed quickly by rotary evaporation at about 60°C to prevent preferential precipitation of the less soluble component. The sample was then scraped into an 8 mm NMR tube. The first sample (53 mol%) contained roughly 15 mg of labelled lipid and had a total lipid mass of 23 mg. This sample was hydrated in about 300 μl of 50 mM phosphate buffer at pH 7.0. Following the series of NMR measurements, the hydrated sample was recombined with the residue in the original flask and the water removed by rotary evaporation from ethanol several times. Using the known

sample composition, the amount of each lipid in the flask was calculated. The amount of SOPC needed to obtain the next desired composition was determined and added to the flask. The components were then redissolved in ethanol and the process repeated. For all samples following the first, the NMR samples were hydrated in distilled water to avoid increasing the buffer concentrations. The samples with the three highest concentrations each contained about 15 mg of labelled lipid. Because of volume limitations the 10 and 5 mol% NMR samples contained only 5.4 mg and 3.2 mg, respectively, of the labelled lipid.

^{2}H-NMR spectra were collected starting from 76°C for the samples containing 53 mol%, 35 mol% and 24 mol% glycolipid, and from 70°C for the remaining samples. The high starting temperature was chosen in order to facilitate equilibrium distribution of components in the bilayer. The small amounts of labelled lipid present required relatively long collection times for each spectrum. In order to reduce the exposure of each sample to high temperatures, spectra were generally collected at 3°C intervals. For the lowest two concentrations, spectra were collected at 9°C intervals in the highest temperature range (more than 20°C from the expected liquidus), 1°C intervals in the region of two phase coexistence, and 3°C intervals otherwise. GalCer and mixtures containing GalCer are known to exhibit hysteresis in their thermal behaviour [16–18,22]. Fast cooling of *N*-(lignoceroyl)GalCer and its mixtures with DPPC from the liquid crystalline phase has been found to result in metastable gel phases [16,18]. For mixtures with phosphatidylcholine, fast cooling might also limit lateral redistribution of bilayer components and further prevent the attainment of equilibrium. In the present work, samples were equilibrated above the main transition temperature of each sample for at least an hour. Because of the averaging time necessary to collect each spectrum, subsequent cooling occurred at a rate between 0.5 and 1 °C per hour: this is relatively slow compared to cooling rates employed in the previously mentioned published studies. While it does not totally preclude the possibility of metastable gel phase formation, this cooling protocol is expected to contribute to the maintenance of sample equilibrium as the temperature is lowered.

^{2}H-NMR spectra were collected at 23.215 MHz using the quadrupole echo sequence [23]. The $\pi/2$ pulse length was between 2.1 μs and 2.3 μs. Pulse separation in the echo sequence was 35 μs. The signal-to-noise ratio of the free induction decay was improved by oversampling by a factor of two, applying symmetrization and smoothing to even and odd points separately, and recombining the echoes in the manner described by Prosser et al. [24]. Effective digitizer dwell time was thus 4 μs in the liquid crystalline phase and 2 μs for temperatures below the liquidus. For each spectrum, 12000 to 48000 transients were collected with a repetition time of 0.6 s. ^{2}H-NMR difference spectroscopy [12–14] was used to determine tie line endpoints in selected two phase regions of the phase diagram for the GalCer(d_{47})/SOPC mixture.

Results and Discussion

Fig. 1 shows ^{2}H-NMR spectra for five sample compositions from 5–53 mol% GSL at 1°C, 10°C, 16°C, 25°C, 40°C, and 70°C. Spectra of long chain perdeuterated fatty acids in common chain length (i.e. shorter) phospholipid matrices have not been reported previously; however, certain inferences may be drawn by inspection based upon experience with phospholipids and sphingolipids having 14–18 carbon deuterated fatty acids. In approaching the analysis of GalCer behaviour in SOPC, we first examined the spectra under several limiting sets of conditions – where one form or another of the GSL (i.e. one molecular arrangement or another) might be expected to predominate. Thus all of the glycolipic spectra above the liquidus (for example at 70°C) display clear evidence of axially symmetric molecular motion, as expected for a perdeuterated chain in a liquid crystalline phase. However, they differ from the usual (shorter) chain-perdeuterated pure liquid crystal spectrum (which might be seen with a phosphatidylcholine [25–27] or GSL [28] in a membrane of homogeneous chain length), in that there is greater concentration of intensity toward the centre of the spectrum, and the splitting associated with the methyl group at the end of the chain is barely resolved. This type of spectrum has been reported recently for small concentrations of DSPC with perdeuterated fatty acids in undeuterated DMPC [14] – which is also a case of a longer labelled chain incorporated into a bilayer whose thickness is determined primarily by a shorter chain lipid. In the absence of a complete analysis, it seems reasonable to assume that the buildup of intensity near the centre is associated with GSL fatty acid methylene groups toward the methyl terminus. Given this assumption, since spectral splittings decrease with decreasing orientational order, the appearance of the liquid crystal spectra would suggest that the extra length of the 24-carbon glycolipid chain manifests relatively low orientational order toward the methyl terminus.

There appear to be two types of ordered phase spectra. The first is associated with small concentrations of *N*-(lignoceroyl)GalCer in SOPC: an SOPC-rich phase which we shall refer to as G_1. It is seen in Fig. 1 for mole fraction 0.05 at 1°C. The ^{2}H-NMR spectrum of the G_1 phase differs from the usual gel phase spectrum observed for shorter chain phospholipids [25–27], in that there is greater buildup of intensity near the centre of the spectrum. This implies that in

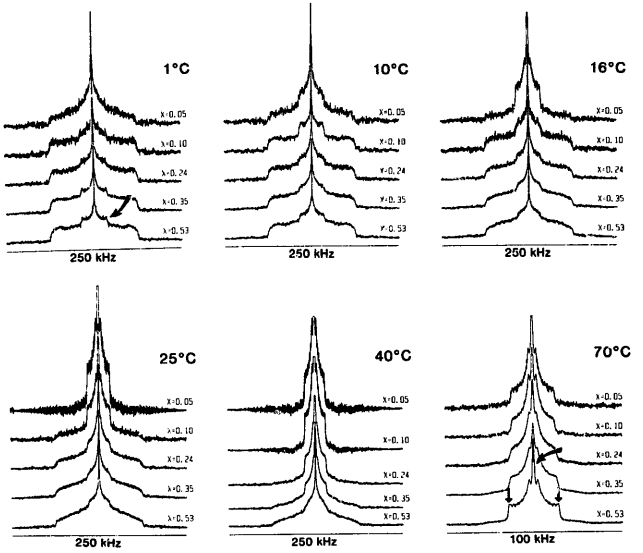

Fig. 1. Concentration dependence of ^{2}H-NMR spectra for *N*-(lignoceroyl-d_{47})GalCer in SOPC at the temperatures indicated from 1°C to 70°C. Curved arrows in the 1°C and 70°C spectral groupings indicate features associated with the 24-carbon fatty acid terminal methyl referred to in the text with regard to G_2 and liquid crystal phases, respectively. Vertical arrows in the 70°C spectral group indicate the liquid crystal plateau region edges.

G_1, the longer chain again appears to be accommodated with some disordering near the methyl end.

The other ordered phase, which we have designated G_2, appears to be nearly pure *N*-(lignoceroyl)GalCer. In spectra obtained from glycolipid/SOPC mixtures, it was always superimposed with either the liquid crystalline spectrum or the G_1 spectrum. However, the G_2 spectrum could be obtained in isolation by using spectral subtraction as described below. The glycolipid studied has one long alkyl chain (the 24-carbon fatty acid), and a shorter chain provided by the sphingosine backbone that extends some 14 or 15 carbons from the membrane surface. Hence, if G_2 is nearly pure glycolipid, it seems reasonable to suggest that the long chain can be readily accommodated by 'partial interdigitation', as has been described for pure single component mixed chain phospholipids and sphingolipids [15,16, 29–33]. It displays some features characteristic of the rigid lattice spectrum [26] below 40°C. In particular, the prominent (methyl) feature with a width of about 34 kHz can be seen in lower temperature spectra. It is this feature which can be used to distinguish G_1 and G_2 components in spectral analysis.

In order to test the above suggestion that the G_2 spectrum represents a phase highly enriched in GalCer, in a separate experiment spectra were collected for a small sample of pure *N*-(lignoceroyl-d_{47})GalCer at a series of temperatures (Fig. 2A). Since the transition temperature of the pure species is at the upper limit of the temperature range supported by our controller, this sample was equilibrated at its initial highest temperature somewhat differently than the mixed samples which form the major body of this work (outside the probe, see figure caption). Despite slow cooling, the pure hydrated lipid showed some indication of non-equilibrium behaviour. Although (non-deuterated) *N*-(lignoceroyl GalCer has a main transition temperature of 82–85°C, at 75°C the sample displayed a liquid crystalline spectrum with evidence of significant disordering near the methyl terminus (Fig. 2A). This is

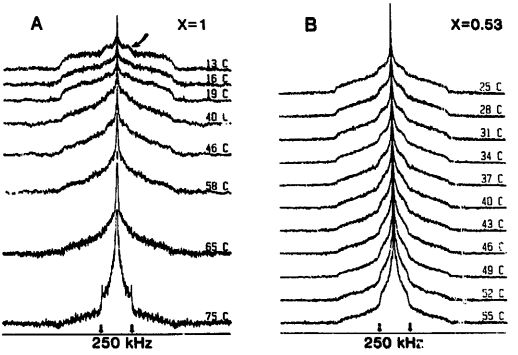

Fig. 2. Temperature dependence of ^{2}H-NMR spectra for: (A) pure *N*-(lignoceroyl-d_{47})GalCer in hydrated bilayer form, and (B) *N*-(lignoceroyl-d_{47})GalCer in SOPC at glycolipid mol fraction $x = 0.53$. The pure GSL sample comprised 7 mg of lipid dispersed in an excess of buffer, frozen and then warmed to 90°C twice before being incubated at 90°C for 1 h. The sample temperature was then lowered to 75°C in several steps over a 6 h interval, following which it was transferred to the NMR probe which had been preheated to 75°C. Each spectrum in A is an average of between 12000 and 36000 transients collected with a repetition time of 0.6 s. Cooling of this sample from 75°C to 50°C proceeded at an effective rate of about 0.6 C°/h. Other experimental conditions were as described in Materials and Methods. Vertical arrows indicate ±17 kHz on the frequency axis. The curved arrow in (A) indicates the methyl feature referred to in the text.

likely a result of the known slightly lower transition of perdeuterated lipids, and the supercooling phenomenon recorded by Reed and Shipley [16]. A very narrow (less than 5 kHz wide) central peak persisted along with the more ordered spectra at lower temperatures. The size of this feature was found to depend on the thermal history of the sample, suggesting that it reflects the presence of molecules in the sample which failed to attain their most ordered packing array as molecular motion was reduced through sample cooling. The spectra of the pure GSL in bilayer form are consistent with the description of the G_2 phase referred to above. The shoulders at about ±17 kHz in the lower temperature spectra are assigned to the fatty acid methyl group. Methyl deuterons constitute 6.5% of the label atoms in this glycolipid. Because of the longer T_{2e} typical of methyl deuterons, they might be expected to account for a somewhat higher proportion of the spectral intensity. In the 16°C spectrum the feature with shoulders at ±17 kHz accounts for about 10% of the intensity. The much narrower feature on top of the methyl spectrum accounts for about 2% of the total intensity, which is too small to correspond to any of the expected resonances. This signal is thus likely to arise from a small fraction of the sample in a non-equilibrium state.

All of the spectra observed can be identified as corresponding to one of G_1, G_2, or fluid phase, or to a superposition of two of these. It should thus be possible to construct a phase diagram, consistent with spectral data, involving these three phases. As will be discussed below, where two or more such spectra at a given temperature are superpositions of the same spectral components, quantitative spectral differences can be used to separate these components and to obtain the sample compositions corresponding to the boundaries of the two phase coexistence region at that temperature. Preliminary estimations of the phase boundary locations can be obtained by inspection of the spectra and by examining the dependence of the first spectral moment on temperature and sample composition.

The first moment, M_1, of a spectrum is obtained as a weighted average of the splittings [26]. In the liquid crystalline phase, M_1 is directly proportional to the mean orientational order parameter for the chains,

$$\bar{S}_{CD} = \langle(\tfrac{1}{2})(3\cos^2\Theta_{CD} - 1)\rangle$$

where Θ_{CD} is the angle between the CD bond and the bilayer normal, and averages are taken over the motions of each CD bond and over all of the deuterons contributing to the spectrum [26]. Non-axially symmetric motion in the ordered phases complicates the interpretation of M_1 in these phases but it can still be assumed to increase with increasing orientational or-

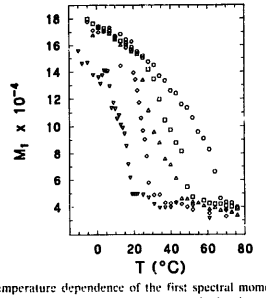

Fig. 3. Temperature dependence of the first spectral moment, M_1, for *N*-(lignoceroyl-d_{47})GalCer in SOPC at mole fractions $x = 0.53$ (○), $x = 0.35$ (□), $x = 0.24$ (△), $x = 0.10$ (◇), and $x = 0.05$ (▽).

der. Fig. 3 shows plots of M_1 vs. temperature for the five samples studied. The liquidus temperature for each sample can be identified as the temperature at which M_1 departs from its nearly constant high temperature value. The approximate convergence of M_1 between 20°C and 30°C for the four samples with highest *N*-(lignoceroyl)GalCer concentrations, suggests the existence of a horizontal or nearly horizontal boundary in this temperature range. Low temperature values of M_1 for the four samples with the highest glycolipid concentrations are very high and suggest nearly-rigid lattice spectral components. The fact that the lowest concentration sample displays a different behaviour suggests that it falls outside the temperature range in which one of the coexisting phases is very highly ordered with a nearly-rigid lattice spectrum.

In order to proceed further in the analysis, it was necessary to identify individual spectral components in cases in which there were coexisting phases. Below the liquidus line this was complicated by the fact that the 34 kHz width of the methyl feature in the G_2 spectrum is nearly the same as the separation of the liquid crystal 90° edges (prominent outer edges associated with plateau-region deuterons of alkyl chains in liquid crystal membranes oriented with their bilayer normals perpendicular to the magnetic field [25–27]). Some indication as to which feature is giving rise to intensity in this region of the spectrum can be obtained by observing its temperature and concentration dependence. The intensity of the liquid crystalline feature should decrease with decreasing temperature and with increasing glycolipid concentration. The behaviour of the ordered methyl feature should be just the opposite. This situation is illustrated in Fig. 2B which shows the temperature dependence of the spectra for $x = 0.53$ between 55°C and 25°C. As will be demonstrated below, the spectra in this region should be superpositions of liquid crystal and G_2 spectra. At 55°C, the dominant feature between ± 17 kHz is clearly liquid crystalline. As the temperature is lowered, the liquid crystal contribution to the spectrum decreases and the intensity of the ordered methyl feature, presumably, increases. At 40°C, the prominent liquid crystal edges at ± 17 kHz have nearly been replaced by the triangular feature, of nearly the same width, associated with the ordered methyl group in the G_2 phase. The very narrow central peak seen in the liquid crystal spectrum remains visible. As the temperature is lowered further, the ordered methyl feature becomes increasingly prominent as it approaches its rigid lattice shape. This interpretation is consistent with the results of spectral subtraction presented below.

Having tentatively identified spectral components that characterise each of the three phases in coexisting mixtures, it is possible to address in more detail the features of the phase diagram. Based both on inspection of the spectra and on the temperature dependence of M_1, the liquidus curve can be taken to run from about 20°C at $x = 0.05$ to 65°C at $x = 0.53$. It can be presumed to meet the SOPC axis at the SOPC main transition temperature of 6–7°C and the GalCer axis at about 80°C. Below 4°C, the $x = 0.05$ spectrum appears to be G_1 only, whereas the spectra for $x = 0.24$, $x = 0.35$ and $x = 0.53$ appear to be superpositions of G_1 and G_2. Between 4°C and 20°C, the interpretation is somewhat more difficult. While the spectra for the three highest concentrations at 10°C and 16°C (Fig. 1), do show a narrow central component, the earlier discussion of Fig. 2B suggests that the feature with edges near ± 17 kHz is due to methyl deuterons rather than to chains in the liquid crystalline phase. Presumably these spectra are superpositions of G_1 and G_2 spectra. The lower two concentrations at these temperatures (Fig. 1) display a superposition of liquid crystal features with an ordered phase, which must be G_1 based on the above logic. These interpretations are consistent with a peritectic phase diagram having a three phase line near 20°C and a peritectic point between $x = 0.10$ and $x = 0.24$.

Spectral subtraction can be used to test and refine the phase diagram. This approach has been used to provide very detailed determinations of phase boundaries in some cases [12–14]. Within a region of two phase coexistence, on a phase diagram, spectra obtained at a given temperature for different sample compositions must be superpositions of a common pair of endpoint spectra corresponding to the intersection of the isothermal tie line with the boundary of the two phase region. The relative contributions of the two endpoint spectra are controlled by the lever rule. If the spectra are normalized and the endpoint spectra are identifiable, then, for a given temperature, it is possible

to determine what fraction of a spectrum at one composition must be subtracted from a second spectrum at a different composition in order to obtain one of the endpoint spectra. From the fraction which was used in the spectral subtraction it is possible to determine the composition corresponding to the endpoint spectrum, and thus one point on the boundary of the coexistence region in the phase diagram. We will take the mole fractions of labelled lipid in the two measured (and normalized) spectra, S_A and S_B to be x_A and x_B, where $x_A > x_B$. If $S_1 = S_A - KS_B$ is identified as one endpoint spectrum, then the corresponding endpoint composition is given by

$$x_1 = (1 - K)x_A x_B / (x_B - Kx_A) \quad (1)$$

If $S_2 = S_B - K'S_A$ is identified as the other endpoint spectrum, then that endpoint composition is given by

$$x_2 = (1 - K')x_B x_A / (x_A - K'x_B) \quad (2)$$

These expressions ignore differences in transverse relaxation rates between the two phases and assume that the coexisting domains are sufficiently large that exchange of lipids between domains of differing phase can be ignored on the timescale of the quadrupole echo measurement.

In the present experiments, the amount of labelled material available limited the number of concentrations which could be used and the signal which could be obtained with a given sample. A given endpoint can be determined most accurately if the two spectra used in the subtraction are both near that endpoint on the tie line and if both have sufficiently high signal to noise ratio to allow distinguishing features of the component spectra to be identified in the difference spectra. However, the spectra available were sufficient to allow the coexisting endpoint spectra to be identified in different regions of the phase diagram and to confirm the proposed peritectic nature of the phase diagram.

Fig. 4 illustrates subtractions in the liquid crystal-G_2 region of the phase diagram. The spectra, at 40°C, for $x = 0.53$ and $x = 0.35$ yield endpoint spectra corresponding to the G_2 phase at $x = 0.94$ and to the liquid crystalline phase at $x = 0.24$. Using the same two compositions, similar endpoint spectra are obtained at 34°C, 37°C, 43°C and 46°C. The liquid crystal endpoint compositions are consistent with those inferred from the inspection of plots of M_1 versus T. The G_2 endpoint compositions all fall between $x = 0.9$ and $x = 1.0$.

Fig. 5 illustrates subtractions at 13°C for spectra from the same two samples. The G_2 endpoint spectrum is not very different from the spectrum at $x = 0.53$. The other endpoint spectrum, corresponding to $x = 0.23$, is, however, very similar to the G_1 spectrum identified for $x = 0.05$ at 1°C. It is clear that there

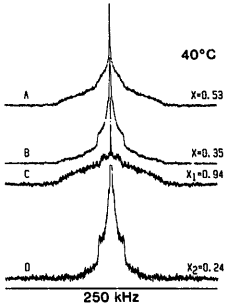

Fig. 4. (A) Spectrum of *N*-(lignoceroyl-d_{47})GalCer in SOPC for $x = 0.53$ at 40°C. (B) Spectrum of *N*-(lignoceroyl-d_{47})GalCer in SOPC for $x = 0.35$ at 40°C. (C) Spectrum obtained by subtracting 0.46 times spectrum B from spectrum A to yield a G_2 phase spectrum corresponding to $x = 0.94$. (D) Spectrum obtained by subtracting 0.59 times spectrum A from spectrum B to yield a fluid phase spectrum corresponding to $x = 0.24$.

exists a region of the phase diagram bounded by G_1 and G_2 and that the $x = 0.53$ and $x = 0.35$ spectra at 13°C contain no liquid crystalline component. By performing subtractions using spectra for the same two compositions, similar endpoint spectra are obtained at

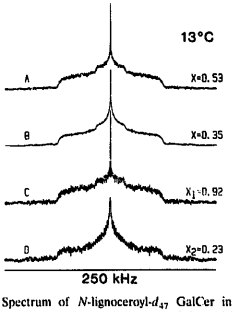

Fig. 5. (A) Spectrum of *N*-lignoceroyl-d_{47} GalCer in SOPC for $x = 0.53$ at 13°C. (B) Spectrum of *N*-lignoceroyl-d_{47} GalCer in SOPC for $x = 0.35$ at 13°C. (C) Spectrum obtained by subtracting 0.45 times spectrum B from spectrum A to yield an ordered phase spectrum corresponding to $x = 0.92$. (D) Spectrum obtained by subtracting 0.6 times spectrum A from spectrum B to yield a spectrum corresponding to $x = 0.23$. Spectrum D suggests less orientational order near the methyl end of the chain than does spectrum C. Spectra C and D are assumed to be characteristic of the proposed G_2 and G_1 phases, respectively.

10°C, 7°C, 4°C and 1°C. These suggest that the boundary between the G_1 and G_1-G_2 regions of the phase diagram is nearly vertical and located near $x = 0.22$. The G_2 boundary appears to remain between $x = 0.9$ and $x = 1.0$.

Fig. 6 illustrates subtractions outside of the G_1-G_2 coexistence region at 13°C. The spectra are very noisy due to the very small amounts of labelled lipid in the $x = 0.10$ and $x = 0.05$ samples. It is clear however, that one component is liquid crystalline and the other ordered. While the poor quality of the ordered endpoint spectrum makes it impossible to distinguish between G_1 and G_2, the fact that it corresponds to a mole fraction less than the lower endpoint of the G_1-G_2 region at that temperature indicates that the coexisting ordered phase must be G_1. A subtraction at 16°C using the $x = 0.05$ and $x = 0.1$ spectra yields similar endpoint spectra and compositions.

The subtractions illustrated in Figs. 5 and 6 indicate that there must be regions of liquid crystal-G_1 and G_1-G_2 coexistence separated by a region of G_1 alone. This information, combined with the type of subtraction illustrated in Fig. 5, implies a peritectic phase behaviour with a three phase coexistence line between about 15°C and 30°C. The phase diagram consistent with all the data presented above is shown in Fig. 7. The points shown as vertical error bars represent the onset of two phase coexistence upon cooling each

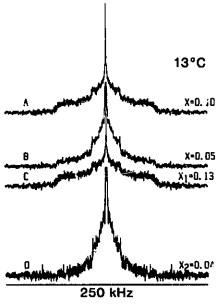

Fig. 6. (A) Spectrum of *N*-(lignoceroyl-d_{47})GalCer in SOPC for $x = 0.10$ at 13°C. (B) Spectrum of *N*-(lignoceroyl-d_{47})GalCer in SOPC for $x = 0.05$ at 13°C. (C) Spectrum obtained by subtracting 0.18 times spectrum B from spectrum A to yield an ordered phase spectrum corresponding to $x = 0.13$. The quality of this subtraction is not sufficient to distinguish between G_1 and G_2 but the calculated endpoint composition falls in the G_1 range determined by the subtraction shown in Fig. 5. (D) Spectrum obtained by subtracting 0.45 times spectrum A from spectrum B to yield the fluid spectral component corresponding to $x = 0.04$.

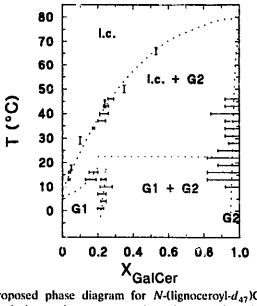

Fig. 7. Proposed phase diagram for *N*-(lignoceroyl-d_{47})GalCer in SOPC. Vertical error bars represent boundary crossings determined by inspection of spectra and consideration of M_1. Horizontal error bars are refinements obtained by selected spectral subtractions. Inspection of spectra below 16°C for $x = 0.10$ suggests that the vertical boundary between G_1 and G_1-G_2, obtained by spectral subtraction, should be displaced toward lower glycolipid concentrations than is shown here.

sample as determined by inspection of the spectra and the behaviour of M_1 versus T. The horizontal error bars represent the results of the subtractions described above. The error in the endpoint composition is subject to and based only on the range of K and K' over which the resulting endpoint spectrum is judged to be acceptable. As no account is taken of the effect of uncertainty in sample compositions, the error bars shown are an underestimate of the true uncertainty. In general, the sensitivity of the endpoint determination to sample composition uncertainty increases rapidly as the separation between the sample and the endpoint compositions increases. The five samples give liquidus temperatures falling along a reasonably smooth curve, which would seem to confirm the quoted sample compositions. The location of the horizontal three phase line shown in Fig. 7 is an estimate based on the behaviour of the boundaries of the G_1 region, and the approximate location of the peritectic point which must exist at the convergence of those boundaries. The data obtained are consistent with the presence of a three phase line anywhere between 20°C and 30°C, but cannot localize it more precisely.

The SOPC host matrix used in the present work was selected to mimic fatty acid features of commonly-occurring phosphatidylcholines in cell membranes. Previously published phase diagrams (derived by DSC) for glycolipids in this phospholipid involved gangliosides from beef brain, with natural fatty acid mixture which is almost totally 18:0 [7]. The phase diagrams derived

for beef brain gangliosides in SOPC are significantly similar to that determined here for the neutral GSL, GalCer, with 24:0 fatty acid: solid phase miscibility was observed below a ganglioside mole fraction of 0.3, with a horizontal solidus at higher GSL concentrations and a wide range of fluid/gel phase coexistence. The DSC study by Curatolo of native beef brain GalCer (which is rich in fatty acid chain lengths from 18 to 24 carbon atoms), in the similar phospholipid, POPC, described the appearance of solid phase immiscibility to even very low GSL concentrations, and a correspondingly wide range of fluid/gel phase coexistence [11]. Once again, peritectic behaviour was not described. Interestingly, the phase diagram determined in the present study of GalCer with 24:0 fatty acid in SOPC is reminiscent of that found by Shipley and co-workers for GalCer with 16:0 fatty acid in DPPC: the latter showed a horizontal solidus above GSL mole fraction 0.2, solid phase miscibility below this GSL concentration, and peritectic behaviour at GSL mole fractions in the range 0.2–0.3 [17]. A reported phase diagram for GalCer with 24:0 fatty acid in DPPC did not find evidence of peritectic behaviour, or solid phase miscibility at low GSL concentration [18].

Conclusions

In spite of shortcomings associated with the presence of limited quantities of deuterated glycolipid in our samples, it was possible to identify the types of phases formed in mixtures of a common naturally-occurring glycosphingolipid and phospholipid in a membrane, and to determine reasonably accurately locations for the phase boundaries. The study was significantly aided by having a spectral probe covalently attached to the glycolipid, and by avoidance of interference from the ice/water phase transition. The same ^{2}H-NMR approach promises to be useful for future work with glycolipids where sample quantity is limited and concentrations in the bilayer are low. An interesting result of being able to examine in detail systems in which GalCer was at low concentration relative to other membrane components, was the observation that the phase behaviour of this glycolipid was importantly different at low vs high concentrations. Above 20 mol% GSL there was solid phase immiscibility of *N*-(lignoceroyl)GalCer, and a strikingly wide range of fluid-rigid phase separation. In contrast, for low GSL concentrations the glycolipid dispersed readily into both solid and fluid phases. Presumably this is a reflection of the fact that, at low GSL concentrations, entropic forces compete effectively with favourable enthalpic interactions amongst like lipids. A similar phenomenon may be seen in the phase diagram for brain gangliosides in SOPC [7]. Relative miscibility of glycolipids at low concentrations in phospholipid based membranes may well be a general expectation, with significance to cell membranes.

Acknowledgements

This research was supported by a grant from the Medical Research Council of Canada to C.W.M.G., and from the National Science and Engineering Research Council to M.R.M.

References

1 Curatolo, W. (1987) Biochim. Biophys. Acta 906, 111–136.
2 Curatolo, W. (1987) Biochim. Biophys. Acta 906, 137–160.
3 Thompson, T.E. and Tillack, T.W. (1985) Annu. Rev. Biophys. 14, 361–366.
4 Grant, C.W.M. (1987) in Gangliosides and Modulation of Neuronal Functions (Rahman, H., ed.), pp. 119–138, NATO ASI Series Cell Biology, Springer-Verlag, Berlin.
5 Maggio, B., Cumar, F.A. and Caputto, R. (1981) Biochim. Biophys. Acta 650, 69–87.
6 Lee, A.G. (1977) Biochim. Biophys. Acta 472, 285–344.
7 Bunow, M.R. and Bunow, B. (1979) Biophys. J. 27, 325–337.
8 Bach, D., Miller, I.R. and Sela, B.-A. (1982) Biochim. Biophys. Acta 686, 233–239.
9 Maggio, B., Ariga, T., Sturtevant, J.M. and Yu, R.K. (1985) Biochim. Biophys. Acta 818, 1–12.
10 Maggio, B., Ariga, T., Sturtevant, J.M. and Yu, R.K. (1985) Biochemistry 24, 1084–1092.
11 Curatolo, W. (1986) Biochim. Biophys. Acta 861, 373–376.
12 Huschilt, J.C. Hodges, R.S. and Davis, J.H. (1985) Biochemistry 24, 1377–1386.
13 Vist, M. and Davis, J.H. (1990) Biochemistry 29, 451–464.
14 Morrow, M.R., Srinivasan, R. and Grandal, N. (1991) Chem. Phys. Lipids 58, 63–72.
15 Davis, P.J. and Keough, K.M.W. (1985) Biophys. J. 48, 915–918.
16 Reed, R.A. and Shipley, G.G. (1987) Biochim. Biophys. Acta 896, 153–164.
17 Ruocco, M.J. and Shipley, G.G and Oldfield, E. (1983) Biophys. J. 43, 91–101.
18 Gardam, M. and Silvius, J.R. (1989) Biochim. Biophys. Acta 980, 319–325.
19 Radin, N.S. (1974) Lipids 9, 358–360.
20 Taketomi, T. and Yamakawa, T. (1963) J. Biochem. 54, 444–451.
21 Kopaczyk, K.C. and Radin, N.S. (1965) J. Lipid Res. 6, 140–145.
22 Reed, R.A. and Shipley, G.G. (1989) Biophys. J. 55, 281–292.
23 Davis, J.H., Jeffrey, K.R., Bloom, M., Valic, M.I. and Higgs, T.P. (1976) Chem. Phys. Lett. 44, 390–394.
24 Prosser, R.S., Davis, J.H., Dahlquist, F.W. and Lindorfer, M.A. (1991) Biochemistry 30, 4687–4696.
25 Seelig, J. (1977) Q. Rev. Biophys. 10, 353–418.
26 Davis, J.H. (1983) Biochim. Biophys. Acta 737, 117–171.
27 Smith, I.C.P. (1984) Biomembranes 12, 133–168.
28 Florio, E., Jarrell, H.C., Fenske, D.B., Barber, K.R. and Grant, C.W.M. (1990) Biochim. Biophys. Acta 1025, 157–163.
29 Keough, K.M.W. and Davis, P.J. (1979) Biochemistry 18, 1453–1459.
30 Levin, I.W., Thompson, T.E., Barenholz, Y. and Huang, C. (1985) Biochemistry 24, 6282–6286.
31 Huang, C. and Mason, J.T. (1986) Biochim. Biophys. Acta 864, 423–470.
32 Mattai, J., Sripada, P.K. and Shipley, G.G.(1987) Biochemistry 26, 3287–3297.
33 Boggs, J.M. and Mason, J.T. (1986) Biochim. Biophys. Acta 863, 231–242.